DOI: 10.1002/ejic.200600492

# Synthesis and Structural Characterization of a New Alkaline Earth Imide: $MgCa(NH)_2$

**Yongfeng Liu,[a] Tao Liu,[a] Zhitao Xiong,[a] Jianjiang Hu,[a] Guotao Wu,[a] Ping Chen,*[a,b] Andrew T. S. Wee,[a] Ping Yang,[c] Kenji Murata,[d] and Ko Sakata[d]**

**Keywords:** Solid-state reactions / Amides / Hydrides / EXAFS spectroscopy / Ternary imide

The ternary imide of $MgCa(NH)_2$ has been successfully synthesized for the first time by the mechanochemical reaction of $Mg(NH_2)_2$ and $CaH_2$ at a molar ratio of 1:1. It was found that ca. four H atoms were desorbed per $Mg(NH_2)_2$-$CaH_2$ after 72 h of ball milling leaving a solid residue with the chemical composition of $MgCa(NH)_2$. The solid residue exhibits an imide N–H stretching vibration at 3151 $cm^{-1}$ and a cubic CaNH-like structure. In addition, X-ray Absorption Fine Structure examination at the Ca *K*-edge indicates that six N atoms occupy the first coordination shell of the Ca center in an anticipated octahedral geometry, and Ca(Mg) atoms occupy the second coordination shell. The distances of Ca–N and Ca–Ca(Mg) in the newly formed $MgCa(NH)_2$ structure calculated by ESDs are 2.46 and 3.47 Å, respectively.


## Introduction

Significant progress in metal nitride research has been made in the past few decades.[1–6] Binary nitrides of the Group 1 and 2 elements, such as $Li_3N$, $Be_3N_2$, $Mg_3N_2$, and $Sr_3N_2$ have been extensively studied[2–3] and used as solar control coatings for windows,[6] reagents for solid-state metathesis reaction,[7–9] and hydrogen storage materials.[10–12] More recently, ternary and multinary nitrides have also been synthesized and investigated due to the unusual crystal and coordination chemistry.[3–6] Unlike nitrides, however, less work has been performed on metal imides. Some basic structural and electronic properties of binary imides such as $Li_2NH$, $Na_2NH$, CaNH, and BaNH are still unknown or controversial.[13–16] As for ternary imides, limited research was done on $Li_2Mg(NH)_2$ and $Li_2Ca(NH)_2$ only in the past two years, motivated by their remarkable hydrogen storage performances.[17–18] Theoretically, the chemical nature of the –NH group enables it to bond with elements from Groups 1–13. A variety of novel ternary or multinary metal imides with unique physical and chemical properties are expected if suitable synthetic routes can be established. Our recent studies showed that a solid-state reaction between metal amides and hydrides could result in the formation of ternary imides. For example, $Li_2Mg(NH)_2$ was synthesized successfully by reacting $LiNH_2$ with $MgH_2$ (molar ratio 2:1) at around 250 °C.[17] The chemical driving force of the above-mentioned solid-state reaction lies in the strong interaction between $H^{\delta+}$ in amide and $H^{\delta-}$ in hydride. However, the thermal instability of the starting amides may lead to self-decomposition at elevated temperatures, which will inevitably result in synthesis failure especially for reactions with slow kinetics. As thermal decomposition of the starting amides is a highly endothermic process, the synthesis of ternary imides may be favored at lower temperature if the overall interaction is mildly endothermic or exothermic. The mechanochemical route, which can perturb surface-bonded species by pressure and enable uniform occurrence of solid-state reaction with poor kinetics at relatively low temperatures,[19–20] could be advantageously used in such synthesis. In this paper, a novel ternary alkaline earth imide, $MgCa(NH)_2$, has been synthesized for the first time by a mechanochemical reaction. FTIR, XRD, and XAFS characterizations were performed to determine the structure of this newly developed imide.

## Results and Discussion

A gaseous product gradually evolved from the mixture of $Mg(NH_2)_2$ and $CaH_2$ (1:1) during the mechanical ball milling treatment, and was identified to be pure hydrogen by a mass spectrometer (Hiden, HPR20). The corresponding amount of hydrogen released from the starting chemicals was calculated by measuring the pressure of hydrogen and the volume of the ball mill vessel. As shown in Figure 1, the amount of hydrogen desorbed increases with ball

[a] Department of Physics, National University of Singapore, 10 Kent Ridge Crescent, Singapore 117542, Singapore
Fax: +65-6777-6126
E-mail: phychenp@nus.edu.sg
[b] Department of Chemistry, National University of Singapore, 10 Kent Ridge Crescent, Singapore 117543, Singapore
[c] Singapore Synchrotron Light Source, National University of Singapore, 5 Research Link, Singapore 117603, Singapore
[d] The Institute of Applied Energy, Shimbashi SY Bldg, 1-14-2 Nishi-shimbashi, Minato-ku, Tokyo 105-0003, Japan

  

milling time. After 12 h ball milling, 11 psi of hydrogen, which is equivalent to ca. 0.5 H atoms per mixture of $Mg(NH_2)_2$–$CaH_2$, was desorbed. After 72 h ball milling, ca. 3.8 H atoms were found to be detached from the mixture. Taking into consideration the purities of the starting chemicals, the number of H atoms released is close to four, being equivalent to the hydrogen storage capacity of ca. 4.0 wt.-%, which is higher than that of most of the traditional metal hydrides, such as $LaNi_5H_6$ (1.4 wt.-%), $FeTiH_{1.9}$ (1.8 wt.-%), and $Mg_2NiH_4$ (3.6 wt.-%). Moreover, EDS analysis reveals that the Mg/Ca atomic ratio in the solid product is 1.03:1, no other metal contamination, such as Fe, was introduced from the stainless steel ball mill jar and balls during the mechanochemical reaction of ball milling.

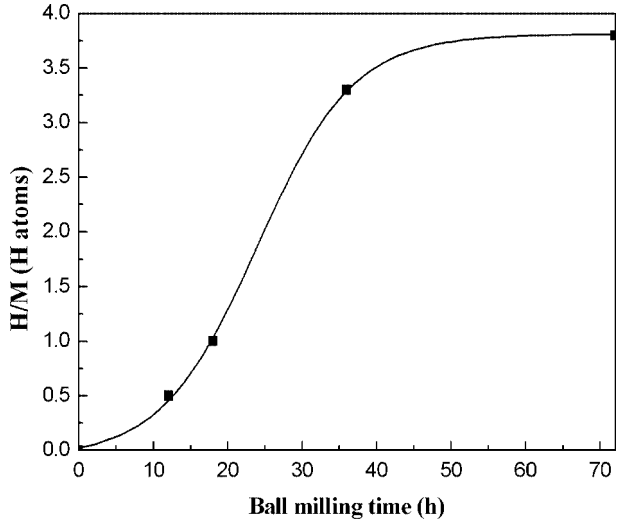


Figure 1. Dependence of the amounts of hydrogen desorption on the ball milling time.

It is well known that $CaH_2$ hardly decomposes to hydrogen at temperatures lower than 600 °C.[21] $Mg(NH_2)_2$, on the other hand, decomposes to $NH_3$ and MgNH at temperatures above 200 °C following the reaction (1).[22–23]

$$Mg(NH_2)_2 \rightarrow MgNH + NH_3 \rightarrow \frac{1}{3}Mg_3N_2 + \frac{4}{3}NH_3 \quad (1)$$

Therefore, hydrogen desorption during the mechanical ball milling should come from the chemical reaction between $Mg(NH_2)_2$ and $CaH_2$ in the present study. Since ca. four H atoms detached from the mixture and no other element was consumed during ball milling, the overall chemical process can be expressed by the following reaction (2).

$$Mg(NH_2)_2 + CaH_2 \rightarrow [MgCa(NH)_2] + 2H_2 \quad (2)$$

The chemical composition of the solid residue indicates that it may be a new ternary imide of Ca and Mg.

It is known that hydrogen atoms in $Mg(NH_2)_2$ are positively charged, while in $CaH_2$ they are negatively charged. The abnormally high enthalpy of the following reaction (3).

$$H^+ + H^- \rightarrow H_2 \ (\Delta H = -17.37 \text{ eV}) \quad (3)$$

is probably the driving force leading reaction (2) to take place under the mechanical ball milling condition.[17] Similar reactions were also observed in other systems such as $LiNH_2$–LiH, $Mg(NH_2)_2$–2LiH, and $LiNH_2$–$CaH_2$ etc. However, it is worth mentioning that it took 72 h for the completion of the reaction under the severe ball milling condition. So the kinetics of the reaction should be very slow. Such slow kinetics will inevitably bring problems to the conventional high temperature synthesis if the starting chemical [like $Mg(NH_2)_2$] or product (the newly developed imide) easily decomposes at elevated temperatures. Therefore, the mechanochemical method developed in the paper could be one of the viable routes for the synthesis of those thermally unstable ternary or multinary imides.

Figure 2 shows the FTIR spectra of the starting chemicals and the solid residues collected at different ball milling times. It can be seen that the N–H symmetric and asymmetric stretching vibrations of $Mg(NH_2)_2$ appear at 3272 and 3326 $cm^{-1}$, respectively. Ca–H vibration in $CaH_2$ is out of the wavenumber range of 3600–2500 $cm^{-1}$. After 12 h ball milling, in addition to the two absorption peaks of $Mg(NH_2)_2$, a broad absorbance at 3151 $cm^{-1}$ was observed, which is located in the N–H vibration range of imide.[13–16] After 72 h ball milling, the characteristic N–H vibrations of $Mg(NH_2)_2$ were almost undetectable. The broad imide-like N–H vibration at 3151 $cm^{-1}$ was enhanced. This result reveals that $Mg(NH_2)_2$ was gradually consumed and an imide-like compound was gradually formed during the ball milling treatment. More importantly, the N–H stretching vibration of the newly developed product of $MgCa(NH)_2$ differs considerably from that of MgNH and CaNH as shown in Figure 2, indicating it is possibly a new ternary imide of Ca and Mg rather than a mixture of MgNH and CaNH.

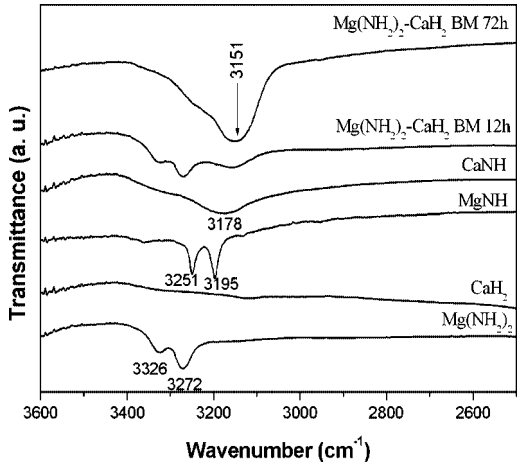


Figure 2. FTIR spectra of the starting chemicals and the Mg–Ca–N–H solid residues after ball milling.

  

Consumption of $CaH_2$ with ball milling was also manifested by the XRD measurements. As shown in Figure 3, the XRD pattern of the post-12 h milled solid residue is mainly composed of the diffraction peaks of orthorhombic $CaH_2$ (refer to the PDF-2 of the JCPDS-ICDD). As $Mg(NH_2)_2$ is easily deformed into an amorphous phase under the energetic ball milling condition,[22] no distinct diffraction peak can be seen. After 72 h ball milling, a new and single phase structure with main diffraction peaks at 30.5, 35.2, and 50.7° was formed (see Figure 3). Matched with the PDF-2 database of the JCPDS-ICDD, the above newly developed solid product possesses a cubic CaNH-like structure. However, compared with CaNH, the diffraction peaks of this product shift to higher angles, revealing a reduction in the unit cell volume. The diffraction pattern is also different from that of MgNH. No other structure assignable to Mg–N or Ca–N can be detected. Combined with the FTIR analyses, it is deducible that this newly developed solid product should be a ternary imide of Ca and Mg, i.e., $MgCa(NH)_2$. Further supportive evidences were obtained from the Temperature-Programmed-Decomposition (TPD) measurements on the $MgCa(NH)_2$, and the mixture of CaNH and MgNH, respectively. Distinct thermal decomposition features were detected. As shown in Figure 4, the solid product decomposes at a peak temperature of 590 °C but the decomposition of the mixture of MgNH and CaNH (1:1) presents two peaks at 650 and 720 °C, respectively.

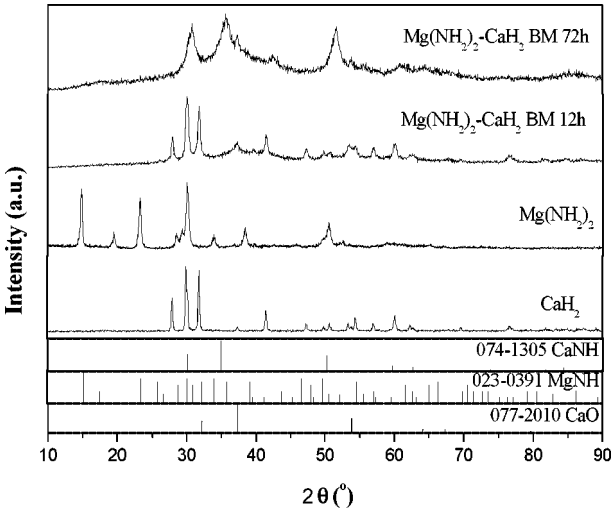


Figure 3. XRD patterns of the starting materials and the Mg–Ca–N–H samples after ball milling.

As can be seen in Figure 3, however, the newly developed imide exhibits rather broad diffraction peaks revealing poor crystallinity in the sample, which is the consequence of the long mechanical ball milling treatment. Because of the poor crystallinity, local structural information could not be convincingly derived from XRD data. The thermal instability of the imide [$MgCa(NH)_2$ decomposes to $NH_3$ at temperatures above 350 °C] defeated our attempt on sample annealing. In order to obtain more structural information on the

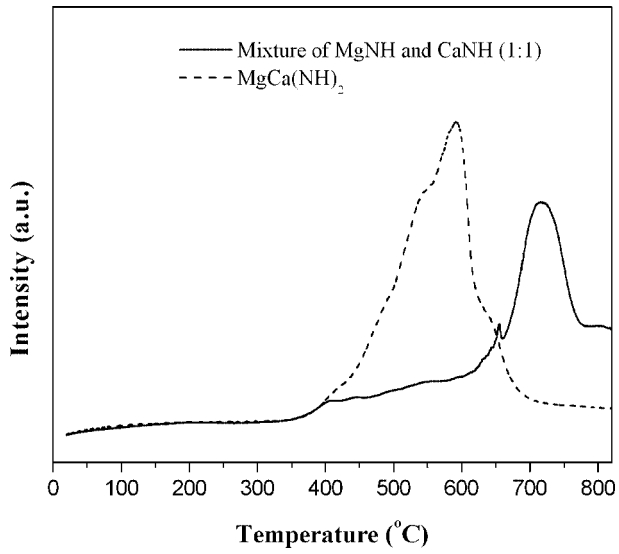


Figure 4. TPD behavior of $MgCa(NH)_2$ and the mixture of MgNH and CaNH.

novel ternary imide, XAFS measurements were conducted. Data of Ca *K*-edge of CaO, CaNH, $Ca(NH_2)_2$, and $MgCa(NH)_2$ were collected and analyzed.

Figure 5 shows the XANES spectra of CaO, CaNH, $Ca(NH_2)_2$, and $MgCa(NH)_2$ samples at Ca *K*-edge, respectively. Obviously all samples exhibit similar spectral features, revealing that they possess the octahedral geometry local structure.[24] Four features can be identified and labeled as A, B, C, and D in Figure 5. Peak A at 4.039 keV can be assigned to the characteristic electron transition from 1*s* to 3*d*.[25] This quadruple transition is usually very weak. However, it is enhanced by the deviation from local centrosymmetry with respect to the central atom (Ca). Compared with CaO, peak A is more obvious in $MgCa(NH)_2$, indicating that the Ca–N octahedrons are somehow distorted. As Mg is more likely to partially replace Ca positions in the second neighboring shell of Ca, the mismatch of atomic radii may result in the distortion of the Ca–N octahedrons. The peak B at 4.042–4.044 keV and peak C at 4.050 keV are ascribed to the dipolar $1s \rightarrow 4p$ transition.[26] Peak B is usually sharp for perfect octahedral sites as shown in CaO.[27] The asymmetry of peak C could be due to the nonequivalent $p_x$, $p_y$, and $p_z$ orbitals of Ca bonded to neighboring nitrogen atoms. Peak C for $MgCa(NH)_2$ shows a shift towards higher energy from 4.049 to 4.050 keV, an indication of a reduced distance between Ca and N compared with that of CaNH. Peak D at 4.058–4.062 keV is related to a middle range ordering as previously demonstrated.[27] Comparatively the ternary $MgCa(NH)_2$ has less middle range ordering, which may be due to its poor crystallinity.

EXAFS looks only at the radial structures of coordination shells around the absorbing atoms. N or O atoms sit in the first coordination shell surrounding the Ca center, and Ca or Mg atoms occupy the second coordination shell. Figure 6 (a) shows Fourier transformed spectra of the various Ca-containing samples. The first peak is assigned to the distance between Ca and the atoms in the first coordination

  

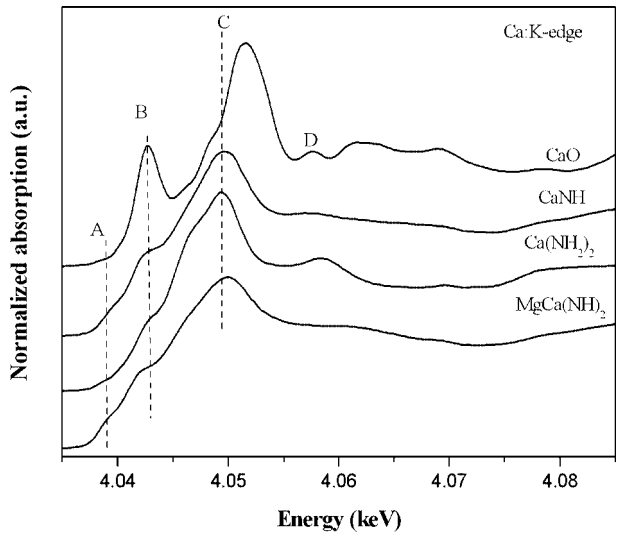


Figure 5. XANES transmission spectra at Ca *K*-edge of the CaO, CaNH, $Ca(NH_2)_2$, and $MgCa(NH)_2$ samples.

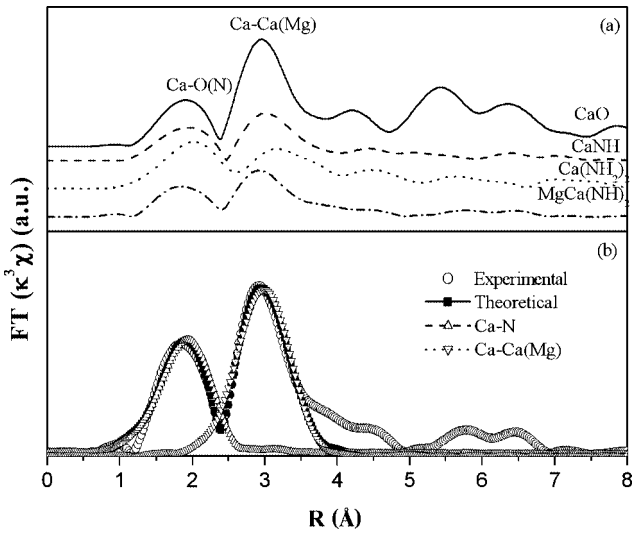


Figure 6. Fourier transformations of the EXAFS spectra of the various Ca-containing samples. (a) Experimental data; (b) fitting results.

shell, i.e., Ca–N or Ca–O; the second peak is attributed to the distance between Ca and the atoms in the second coordination shell, i.e., Ca–Ca and/or Ca–Mg. It should be noted that EXFAS cannot distinguish the positions of Ca and Mg in the second coordination shell of the Ca center. Ca and Mg are more likely to evenly occupy the octahedral center of N in the lattice to minimize energy. Two to three peaks can be identified arising from higher order shells. Figure 6 (b) shows the experimental data and fitting result of $MgCa(NH)_2$, which shows good agreement in the range of 1 to 4 Å. Similar fitting was also performed on CaNH and $Ca(NH_2)_2$, and the results are summarized in Table 1. It is noted that the coordination number (N) of Ca in the first coordination shell is close to 6 for all samples, indicating that octahedral geometry is retained in the first coordination shell, in good agreement with the XRD results. However, the coordination numbers of the second coordination shell are obviously lower than the actual values due to the disorder effects at high coordination shells. Meanwhile, it should be noted that the value of $Ca(NH_2)_2$ (4.4) is lower than that of $MgCa(NH)_2$ (8), which can be attributed to the vacancies of Ca in the second coordination shell due to the lower ratio of the metal atom and N atom (1:2) in the $Ca(NH_2)_2$ structure compared to that in the $MgCa(NH)_2$ structure (1:1).[13] The Ca–N and Ca–Ca distances of CaNH are calculated to be 2.49 and 3.53 Å, respectively, which match well with the values (Ca–N: 2.50 Å, Ca–Ca: 3.54 Å) obtained from the known crystallographic data. On the other hand, the Ca–N and Ca–Ca(Mg) distances of $MgCa(NH)_2$ are calculated to be 2.46 and 3.47 Å, respectively, which are the shortest among the three Ca–N-based structures in the present study. This contraction of atomic distances is in good agreement with the reduction of lattice parameters detected by XRD, which is probably due to the smaller ionic radius of Mg (0.72 Å) compared to Ca (1.0 Å).

Table 1. Structural parameters of CaNH, $Ca(NH_2)_2$, and $MgCa(NH)_2$ obtained from XAFS.[a,b]

| Sample | Shell | Coordination | R [Å] | *N* | $\sigma^2$ [Å$^2$] | Residual [%] |
|---|---|---|---|---|---|---|
| CaNH | 1 | Ca–N | 2.49 | 6.0 | 0.0173 | 9.2 |
| | 2 | Ca–Ca | 3.53 | 6.4 | 0.0132 | |
| $Ca(NH_2)_2$ | 1 | Ca–N | 2.51 | 6.7 | 0.0130 | 16.0 |
| | 2 | Ca–Ca | 3.67 | 4.4 | 0.0078 | |
| $MgCa(NH)_2$ | 1 | Ca–N | 2.46 | 5.9 | 0.0118 | 10.6 |
| | 2 | Ca–Ca(Mg) | 3.47 | 8.0 | 0.0174 | |

[a] Error bars for *R* are 0.01 Å, for *N* and $\sigma^2$, 10%. [b] Data fitting does not include the effects of the H atoms and the oxide contamination.

According to the above discussions, it can be seen that the newly formed ternary imide of $MgCa(NH)_2$ possesses a CaNH-like cubic structure. The half substitution of Ca by Mg does not substantially change the lattice configuration of CaNH, but the lattice has shrunk considerably compared with CaNH, because of the smaller ionic radius of Mg. Figure 7 illustrates a structural model of $MgCa(NH)_2$, in which Ca(Mg) occupies the 4a site (0,0,0) and N occupies the 4b site (1/2,1/2,1/2) of space group Fm-3m, and the N atoms sit in the octahedral holes made of Ca(Mg). However, it is difficult to determine the position of H in the ternary imide by means of XRD and XAFS. There are a number of investigations on the position of H in binary imides, such as CaNH and BaNH.[16,28] As Jacobs et al. pointed out the NH group in CaNH is dynamically disordered at room temperature, and the maximum possibility for the location of hydrogen is the eightfold split position along <111> directions in Ca-octahedra.[16,28] In other words, there are eight possible positions for the H atoms in the structure of CaNH, and every H atom points to the relevant face of the octahedron of Ca. According to the XRD and XAFS analyses, the crystal structure of the newly formed

  

$MgCa(NH)_2$ resembles that of CaNH. Therefore, it is suggested that the situation of the H atoms in $MgCa(NH)_2$ is similar to that in CaNH as shown in Figure 7.

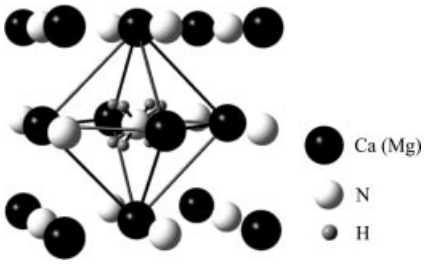


Figure 7. Structural model of $MgCa(NH)_2$.

## Conclusions

In this paper, a novel ternary alkaline earth imide has been synthesized by the mechanochemical reaction of $Mg(NH_2)_2$ and $CaH_2$ with a molar ratio of 1:1. The newly formed ternary imide of $MgCa(NH)_2$ has a CaNH-like cubic structure. Mg atoms partially substitute Ca atoms in the lattice resulting in a distorted local centro-symmetry and poor near and middle range ordering. The Ca–N and Ca–Ca(Mg) distances of $MgCa(NH)_2$ were calculated by ESDs to be 2.46 and 3.47 Å, respectively.

## Experimental Section

All samples were handled in a glovebox (MBRAUN) filled with purified argon ($H_2O$: <1 ppm, $O_2$: <1 ppm). The starting chemicals for the mechanochemical reaction were $Mg(NH_2)_2$ and $CaH_2$. $Mg(NH_2)_2$ was synthesized by reacting pre-milled metallic Mg (99%, Riedel-De Haen) with $NH_3$ (99.98%, BOC GASES) at 300 °C, and its purity was estimated by XRD analyses and measured by thermogravimetric methods, i.e., by measuring the weight loss of a $Mg(NH_2)_2$ sample during the thermal decomposition. Only the diffraction patterns of $Mg(NH_2)_2$ can be detected by XRD examination; and the weight loss was 39.7% as the self-made $Mg(NH_2)_2$ was heated from 25 to 720 °C. The theoretical weight loss was 40.5% when $Mg(NH_2)_2$ was decomposed to $Mg_3N_2$ and $NH_3$. Thus, the purity of the self-made $Mg(NH_2)_2$ is about 98%. $CaH_2$ powder with 95% purity was purchased from Sigma–Aldrich. The mechanochemical reactions were performed on a Retsch PM400 planetary ball mill. In a typical procedure, the starting chemicals of $Mg(NH_2)_2$ (1.4 g) and $CaH_2$ (1.05 g) (molar ratio 1:1) were mixed and then milled at 200 rpm. The ball milling treatment was stopped at different intervals (12–72 h) to measure the pressure changes within the ball mill vessel. After 72 h of mechanochemical reaction, the sample was collected and weighed. Although some of the product adhered to the milling balls and the inner surface of the ball mill vessel, ca. 2.2 g of gray powder was ultimately obtained. The Mg/Ca atomic ratio in the solid product was examined by EDS with a Philips XL30 Scanning Electron Microscope (SEM).

The thermal decomposition of the solid product and the mixture of MgNH and CaNH was carried out with the home-made Temperature-Programmed-Decomposition (TPD) system with an online mass spectrometer (MS) and gas chromatograph (GC) attached. Argon was used as the carrier gas. About 100 mg of sample was loaded and tested each time. The temperature was raised gradually from 20 to 820 °C at 2 °C/min.

N–H vibrations of all samples were detected with a Perkin Elmer FTIR-3000 unit in DRIFT mode. The phase identification was carried out by X-ray diffraction (XRD). A Bruker D8-advance X-ray diffractometer with Cu-$K_\alpha$ radiation at 40 kV and 40 mA equipped with an in-situ cell was used. X-ray absorption fine structure (XAFS) experiments at the Ca *K*-edge (4.038 keV) were performed in transmission mode at room temperature at the XDD beamline in the Singapore Synchrotron Light Source (SSLS).[29] CaO, CaNH, and $Ca(NH_2)_2$ were used as reference samples measured under the same experimental conditions. CaO with 99.9% purity was purchased from Sigma–Aldrich; $Ca(NH_2)_2$ was synthesized by reacting metallic Ca (98.5%, Merck) with $NH_3$ at room temperature.[30] CaNH was obtained by the thermal decomposition of $Ca(NH_2)_2$.[13,31] Each sample was pressed into a pellet by mixing with LiF powder (99%, Fluka) in a weight ratio of 1:10 under a pressure of 2.5 tons; the pellets were subsequently coated with solid wax under an inert atmosphere to protect against air contamination during XAFS measurements. The thickness of the samples was adjusted to achieve a jump of about 1 in absorption coefficient at the absorption edge. Ca *K*-edge XAFS spectra were analyzed following the standard methods using the WINXAS code.[32] The extracted $\chi(k)$ in the range 2.2–9.2 $Å^{-1}$ was weighted by $k^3$ and Fourier transformed into *R* space using the Bessel window function. Data fitting was performed in *R* space without considering the effects of H atoms by filtering out the first and second coordination shells. The other possible error may be generated from the impurities of the reference sample. For all systems, we used the amplitude reduction factor of $S_0^2 = 0.73$, a theoretical value extracted from the fit of CaNH by fixing the known crystallographic data.

## Acknowledgments

We would like to acknowledge the financial support from the Agency for Science, Technology and Research (A*STAR Singapore) and the New Energy and Industrial Technology Development Organization (NEDO, Japan) under the International Joint Research Project "Development for Safe Utilization and Infrastructure of Hydrogen". We also would like to thank Prof. H. O. Moser, SSLS, for discussion and suggestions.

[1] P. Eckerlin, A. Rabenau, *Z. Anorg. Allg. Chem.* **1960**, *304*, 218–219.
[2] O. Reckeweg, F. J. DiSalvo, *Z. Anorg. Allg. Chem.* **2001**, *627*, 371–377.
[3] D. H. Gregory, *Coord. Chem. Rev.* **2001**, *215*, 301–345.
[4] R. Niewa, F. J. DiSalvo, *Chem. Mater.* **1998**, *10*, 2733–2752.
[5] D. H. Gregory, *J. Chem. Soc. Dalton Trans.* **1999**, *3*, 259–270.
[6] P. F. Henry, M. T. Weller, *Angew. Chem. Int. Ed.* **1998**, *37*, 2855–2857.
[7] O. Reckeweg, C. Lind, A. Simon, F. J. DiSalvo, *Z. Naturforsch. Teil B* **2003**, *58*, 159–162.
[8] L. Rao, R. B. Kaner, *Inorg. Chem.* **1994**, *33*, 3210–3211.
[9] E. G. Gillan, R. B. Kaner, *Chem. Mater.* **1996**, *8*, 333–343.
[10] P. Chen, Z. T. Xiong, J. Z. Luo, J. Y. Lin, K. L. Tan, *Nature* **2002**, *420*, 302–304.
[11] Z. T. Xiong, P. Chen, G. T. Wu, J. Y. Lin, K. L. Tan, *J. Mater. Chem.* **2003**, *13*, 1676–1680.
[12] Y. Kojima, Y. Kawai, *Chem. Commun.* **2004**, 2210–2211.
[13] R. Juza, H. Schumacher, *Z. Anorg. Allg. Chem.* **1963**, *24*, 278–286.

  

[14] V. G. Linde, R. Juza, *Z. Anorg. Allg. Chem.* **1974**, *409*, 199–214.
[15] R. Ebmann, H. Jacobs, J. Tomkinson, *J. Alloys Compd.* **1993**, *191*, 131–134.
[16] T. Sichla, H. Jacobs, *Z. Anorg. Allg. Chem.* **1996**, *622*, 2079–2082.
[17] Z. T. Xiong, G. T. Wu, J. J. Hu, P. Chen, *Adv. Mater.* **2004**, *16*, 1522–1525.
[18] W. F. Luo, *J. Alloys Compd.* **2004**, *381*, 284–287.
[19] E. Gutman, *Mechanochemistry of Materials*, Cambridge International Science Publishing, Cambridge, UK, **1997**.
[20] C. Suryanarayana, *Prog. Mater. Sci.* **2001**, *46*, 1–184.
[21] G. G. Libowitz, *The Solid State Chemistry of Binary Metal Hydrides*, W. A. Benjamin, Inc., New York, **1965**.
[22] J. J. Hu, G. T. Wu, Y. F. Liu, Z. T. Xiong, P. Chen, K. Murata, K. Sakata, G. Wolf, *J. Phys. Chem. B* **2006**, *110*, 14688–14692.
[23] Z. T. Xiong, J. J. Hu, G. T. Wu, P. Chen, *J. Alloys Compd.* **2005**, *395*, 209–212.
[24] H. Modrow, S. Bucher, J. J. Rehr, A. L. Ankudinov, *Phys. Rev. B* **2005**, *67*, 035123.
[25] F. de Groot, *Chem. Rev.* **2001**, *101*, 1779–1808.
[26] J. L. Fulton, S. M. Heald, Y. S. Badyal, J. M. Simonson, *J. Phys. Chem. A* **2003**, *107*, 4688–4696.
[27] L. X. Chen, T. Liu, M. C. Thurnauer, R. Csencsits, T. Rahj, *J. Phys. Chem. B* **2002**, *106*, 8539–8546.
[28] B. Wegner, R. Essmann, H. Jacobs, *J. Less-Common Met.* **1990**, *167*, 81–90.
[29] H. O. Moser, B. D. F. Casse, E. P. Chew, M. Cholewa, C. Z. Diao, S. X. D. Ding, J. R. Kong, Z. W. Li, M. Hua, M. L. Ng, B. T. Saw, S. bin Mahmood, S. V. Vidyaraj, O. Wilhelmi, J. Wong, P. Yang, X. J. Yu, X. Y. Gao, A. T. S. Wee, W. S. Sim, D. Lu, R. B. Faltermeier, *Nucl. Instrum. Methods Phys. Res. Sect. B* **2005**, *238*, 83–86.
[30] H. Moissan, *Ann. Chim. Phys.* **1899**, *18*, 289–326.
[31] S. Hino, T. Ichikawa, H. Y. Leng, H. Fujii, *J. Alloys Compd.* **2005**, *398*, 62–66.
[32] T. Ressler, *J. Physique IV* **1997**, *7*, 269–270.

Received: May 27, 2006
Published Online: September 13, 2006

  